Assessing extreme loads on a tidal turbine using focused wave groups in energetic currents

Assessing Extreme Loads on a Tidal Turbine Using Focused Wave Groups in Energetic Currents

S. Draycott[a,*], A. Nambiar[a], B. Sellar[a], T. Davey[a], V. Venugopal[a]

[a]*School of Engineering, Institute for Energy Systems, The University of Edinburgh, Edinburgh, UK, EH9 3DW*

Abstract

Tidal stream turbines are subject to large hydrodynamic loads, including those induced by extreme waves. Scale model testing in the laboratory plays an important role in ensuring that full scale tidal turbines are designed and operated in a manner that is appropriate for harsh ocean environments where waves and tidal currents coexist.

For the first time, a fully-instrumented scaled tidal turbine is tested in short-duration focused wave groups representative of extreme environmental load cases expected at energetic tidal sites. In this paper, the subsequent variations in rotor-based loads, power and blade root bending moments are reported. These measurements are found to strongly follow the spectral and temporal form of the focused wave conditions, and peak loads and power output are found to exceed current-only values by 85% and 200% respectively. These rotor-averaged values display a high level of repeatability, demonstrating the suitability of focused waves for testing seabed-mounted tidal turbines. Extreme blade loads, which are dependent on angular position relative to wave phase, are captured through rapidly obtained repeat tests. New insight is subsequently gained into loading and response of tidal turbines in extreme sea conditions.

Keywords: extreme wave loading, tidal stream turbine, NewWave, focused wave groups, blade bending moments, combined wave-current

1. Introduction

1.1. Understanding environmental loading on tidal turbines

Tidal stream power represents a largely untapped renewable energy source, which is both predictable and reliable. This highly energy-dense power source has the potential to be a major contributor to both European and global energy markets, with recent studies suggesting that in the U.K. alone the theoretical

*Corresponding author
Email address: S.Draycott@ed.ac.uk (S. Draycott)

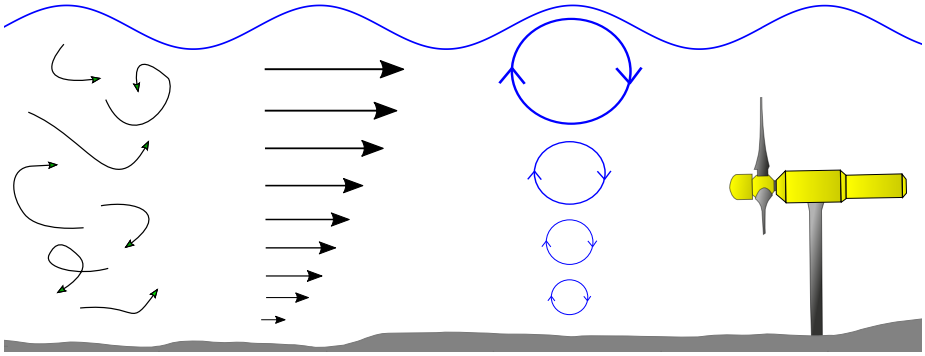

Figure 1: Causes of unsteady loads on tidal turbines. Shown from left to right: turbulence, shear flow and waves

resource is 95 TWh/year [1]. To extract the available power, Tidal Stream Turbine (TST) devices have been actively developed, with the first arrays currently being installed and commissioned [2].

For farms of devices to be viable, TSTs will need to survive large steady and unsteady hydrodynamic loads over their lifetime. Sites with high flow velocities are typically targeted by developers, with notably fast flows occurring in the Pentland Firth, U.K., and at Raz Blanchard, France, which feature peak flows in excess of 5 m/s [3]. Unsteady loads, depicted in Fig. 1, are largely caused by turbulence, waves and shear flow [4, 5, 6]. These all contribute to both fatigue and increased extreme loading on a TST device. The importance of waves at tidal stream power sites is well communicated in industrial standards and guidance documents. The International Electrotechnical Commission (IEC) recommends that waves are considered in resource characterisation process [7], and additionally advises wave measurement programs where wave orbital velocities are likely to be greater than 20% of the rated current speed [8].

1.2. Modelling extreme wave loads

TSTs must contend with velocity fluctuations and loads induced by extreme waves at the deployment site. Hence, the influence of these extreme wave events should be considered in the design process, as indicated by the IEC Technical Specification for design standards for marine energy systems [9].

An attractive experimental approach for the assessment of extreme wave loading is through the generation of a NewWave group [10], designed to provide the statistically most probable shape around the defined extreme wave condition. A NewWave packet consists of a focused short-duration wave group generated from the design wave spectrum, thus giving a polychromatic test environment whilst avoiding the long test durations normally associated with extreme wave testing under irregular sea conditions [11]. The short time-frames provide a further advantage in the wave tank by ensuring wave reflections are not present [12], which may cause significant deviation from the desired and specified wave-induced velocity fields [13, 14].

In this study focused NewWave groups are generated in a following current of 0.8 m/s (corresponding to 3.1 m/s full scale) to assess likely extreme wave-induced loads and power fluctuations of a fully-instrumented, speed controlled, 1:15 scale model tidal turbine. Although NewWave groups have been used in numerous studies assessing extreme loads on offshore structures [10, 15, 16, 17] the applicability to dynamic systems is limited, with only a select number of studies detailing it's use for such applications. Of note, is the application of NewWave groups to assess a wave energy converter (WEC) in [18, 19], and floating production storage and offloading platform (FPSO) in [12]. The presented research represents the first documented application with a tidal turbine and extends the use of the method to faster flow speeds than previously reported, 0.8 m/s as compared to 0.6 m/s in [20]. Tests were conducted at the circular combined wave-current test basin, Flowave, University of Edinburgh (www.flowave.eng.ed.ac.uk).

1.3. Article Layout

In Section 2 the calibration and correction procedure used to create NewWave groups in energetic currents is detailed, along with a description of the 1:15 scale instrumented turbine model, test set-up and test plan. Section 3 details the resulting impact of NewWave groups on turbine parameters including fluctuations in loads, power & blade bending moments. Discussion into the consequences of the results are further developed in Section 4, along with other areas requiring further discussion. Concluding remarks are offered in Section 5.

2. Methodology

2.1. Creating NewWave Groups in Energetic Currents

This section covers both the definition and creation of NewWave groups in the presence of current. Section 2.1.1 covers the spectral definition of specified NewWave groups, whilst Section 2.1.2 details the correction procedure implemented to attain the desired focused wave groups in current.

2.1.1. NewWave Spectral Inputs

A NewWave spectrum provides the most probable extreme surface displacement for a defined wave energy spectrum, $S(f)$. The time-series of this NewWave group can be defined by Eq. (1) [10]:

$$\eta_{NW}(x,t) = \frac{\alpha}{\sigma^2} \sum d_n cos(k_n x - \omega_n t) \tag{1}$$

where $d_n = S(f_n)\Delta f_n$ and Δf_n is the frequency bin width $[Hz]$. α is the crest amplitude $[m]$, x is the position in the direction of wave propagation $[m]$, k is the wave number $[m^{-1}]$, $\omega = 2\pi f$ is the wave angular frequency $[rad/s]$ and σ^2 is the total variance associated with $S(f)$ $[m^2]$.

From Eq. (1) it can be inferred that the complex Fourier coefficients ($a(f)$) required to simulate the NewWave focused event, at streamwise position X

and time t_0, can be described by Eq. (2). This equation describes the target amplitude spectrum at the turbine location and at the time specified. The value of t_0 is determined from the minimum and maximum wave frequencies and wave group focal position, whilst considering the minimisation of reflections. The multiple NewWave groups used and their corresponding values of α, peak spectral frequency f_p and peak spectral enhancement factor γ are described in Section 2.3.

$$a(f) = \frac{\alpha}{\sigma^2} d_n(f) e^{i[k(f)X - w(f)t_0 + \pi]} \tag{2}$$

The input to the FloWave tank is defined in terms of amplitudes and phases for each frequency component, given by:

$$A(f)_{desired} = abs(a(f)) \qquad \Phi(f)_{desired} = atan2[\frac{imag(a(f))}{real(a(f))}] \tag{3}$$

In the absence of current it is possible to convert these to appropriate wavemaker motion spectra (excluding non-linear effects) to re-create the defined wave field effectively. However, wave parameters, including the wave height, wavelength and associated velocities, are significantly altered by the current [21] and, therefore, a correction procedure is required. In addition, current-modified wavenumbers are spatially dependent due to to flow variation in the FloWave tank [22], and as such it is not trivial to identify appropriate $k(f)X$ values to obtain the desired phase. The initial tank input is therefore based on the zero-current calculations, and an iterative procedure is used to obtain the desired conditions.

2.1.2. Iterative Correction Procedure

To iteratively approach the desired spectrum, and the associated NewWave surface elevation, measured values from each iteration are used to define the next input. Measured complex amplitude spectra, obtained from a FFT, provide both the frequency-dependent component amplitudes and phases at the target location. The calculated discrepancies are used to inform the next iteration. The inputs used, for both amplitude and phase at iteration j, are calculated by Eqs. (4) and (5) respectively.

$$A(f)_{in,j+1} = [\frac{A(f)_{desired}}{A(f)_{measured,j}}] A(f)_{in,j} \tag{4}$$

$$\Phi(f)_{in,j+1} = \Phi(f)_{in,j} + \beta[\Phi(f)_{desired} - \Phi(f)_{measured,j}] \tag{5}$$

To aid convergence only a fraction, β, of the total difference between measured and desired phase was used for correction. β values of $\frac{1}{j}$ were found to be effective during these tests and are recommended for use in similar environmental conditions.

2.2. Test Set-up

This section describes the test set-up including a description of the TST model (Section 2.2.1), the FloWave wave-current basin (Section 2.2.2), and the instrumentation layout (Section 2.2.3).

2.2.1. The Model Turbine

The TST model, depicted in Fig. 2, is a 1:15 scale, bed-mounted, fixed-pitch, three-bladed horizontal axis tidal turbine. The rotor diameter, D, is 1200 mm with the turbine rotor axis 1 m from the bed. Being bed-mounted it minimises the disruption to propagating waves, represents a majority of turbines being developed today and also allows for structural loadings on the tower to be measured (as discussed in Section 2.2.3). A detailed description of the design and manufacture of the TST model is given in [23], with recent results of the turbine subject to regular wave conditions presented in [24]. Importantly, it has been designed to incorporate an array of sensors which output rotor-based measurements of torque, Q, thrust, T, and angular position, θ, whilst also providing streamwise root bending moment, RBM, for each blade. These load sensors are placed as close as possible to where the respective loads are being applied, which maximises data quality. Additionally, the blade was designed to produce similar radial variation of the rotor thrust coefficient at a specific tip speed ratio (TSR), when compared to a full scale generic turbine [25]. These turbine design features enables useful conclusions to be extracted from 1:15 scale testing in extreme wave conditions.

The turbine rotor is coupled with a permanent magnet servo motor, which produces a controllable resisting torque to the hydrodynamic torque due to the flow. In this work the motor was set to operate in speed control mode. The speed controller was tuned for the wave conditions tested and was found to maintain speed with a variance between 1.20-1.39% of the reference speed of 90 rpm (nominal TSR of 7).

2.2.2. The Test Facility

All the experimental measurements presented here were made at the FloWave Ocean Energy Research Facility, located at the University of Edinburgh (UoE), U.K. [26] (Figure 3). The facility is a circular, combined wave and current basin, with a diameter of 25 m and a nominal water depth of 2 m. Waves are generated using 168 active-absorbing force-feedback wavemakers around the entire circumference. A re-circulating flow system is generated using 28 impeller units mounted in the plenum chamber beneath the floor [27]. These enable the creation of a predominantly straight flow in any direction across the central test area [22], where waves can be added to the current field at any relative angle.

2.2.3. Instrumentation and Configuration

In addition to the sensors integrated into the TST model (Section 2.2.1), additional instrumentation was installed throughout the test volume as summarised in Table 1. This includes a resistance-type wave gauge to measure

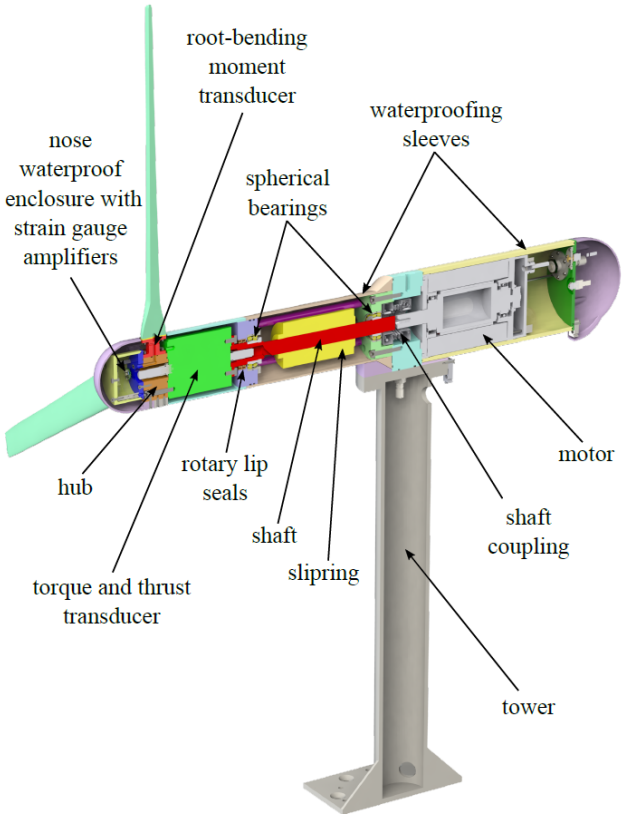

Figure 2: CAD section view of the experimental turbine model [23]

surface elevation, an Acoustic Doppler Velocimeter (ADV) to measure current velocity, and a bottom-mounted six-axes (6-DOF) load cell to measure forces, F, and moments, M, on the entire TST structure (blades, TST body and tower). The test set-up is illustrated in Fig. 4, where the turbine is depicted to scale in conjunction with the installed instrumentation. The location of the ADV was chosen to minimise flow disruption from the instrument and mounting and provide a consistent representative ambient flow condition.

2.3. Test Plan

Three NewWave spectra were defined using Eq. (1) for following current conditions. Tank scale α values of 0.1, 0.15 and 0.2 m were chosen to investigate the TST response to increasing wave amplitudes. $S(f)$ was characterised by a JONSWAP [28] spectrum with a peak frequency, f_p, of 0.4 Hz, and a peak enhancement factor, γ, of 2. Low frequency – narrow bandwidth spectra were used to limit the influence of turbulence on wave repeatability which is further discussed in Section 4.1.2. A focus time t_0 of 16 s was used, with a sea-state repeat time of 32 s (see Eq. (2)). This enables the wave components to arrive

Figure 3: The FloWave Ocean Energy Research Facility.

Table 1: Description of installed instrumentation including position relative to the turbine rotor plane centre

Type	Model	Variables measured	Sample Rate [Hz]	Rel. location [m] X	Y	Z
ADV	Vectrino Profiler	U, V, W	100	-2.40	0	0.60
Wave Gauge	FloWave	η	128	0	0	–
TST Instrumentation	UoE	T, Q, RBM, θ	256	0	0	0
Load Cell	AMTI OR6-7	F_X, F_Y, F_Z, M_X, M_Y, M_Z	256	0.49	0	-1.00

in phase at the turbine location without the influence of reflections. The sea states are summarised in Table 2, along with the full scale equivalent focused wave groups. H^* and T^* are the expected full-scale wave height and period associated with the focused event at t_0.

Table 2: Desired NewWave parameters for tank, and full scale equivalent wave groups.

	Tank Scale			**Full Scale**				
Reference	α [m]	T_p [s]	γ	α [m]	T_p [s]	γ	H^* [m]	T^* [s]
A	0.1	2.5	2	1.5	9.68	2	2.54	8.17
B	0.15	2.5	2	2.25	9.68	2	3.81	8.17
C	0.2	2.5	2	3	9.68	2	5.08	8.17

3. Results

The main findings from the tests are presented in this section. The outputs of the iterative correction without the turbine present are shown in Section 3.1. The time-domain response of the turbine to the NewWave groups is presented in Section 3.2, with spectra of key turbine parameters in Section 3.3. Peak wave-induced loads and power fluctuations as a function of crest amplitude are assessed separately in Section 3.4.

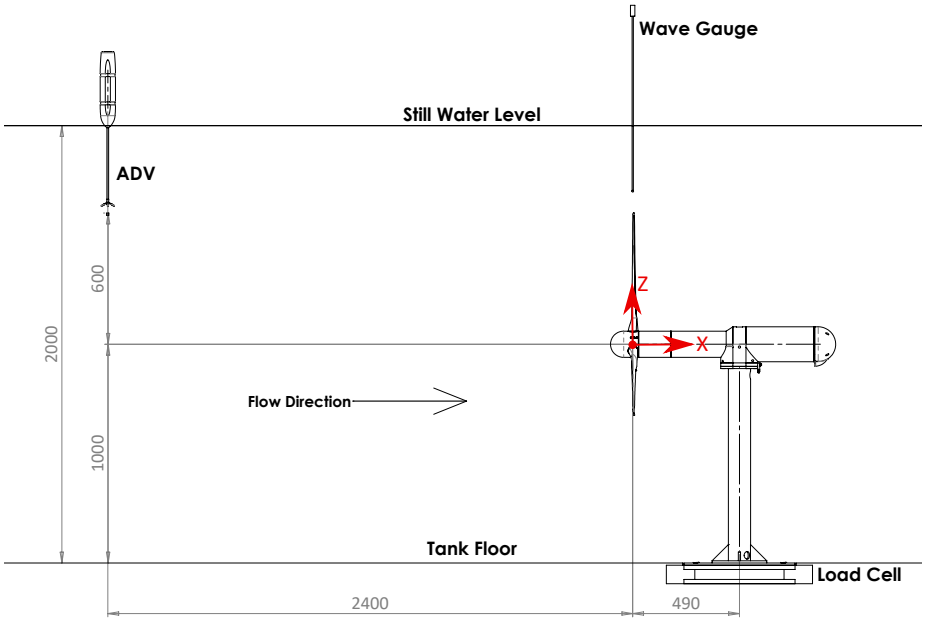

Figure 4: Location of test instrumentation in the FloWave basin relative to the rotor plane (dimensions in mm)

3.1. Iterative Correction Procedure Outputs

The frequency domain iterative correction procedure was carried out as described in Section 2.1.2. After four iterations both the frequency spectra and the time-series of the wave elevation at the turbine location were found to closely match target values. The time domain and the frequency domain results for the initial trial, along with the final 'characterised' conditions are shown in Figs. 5 and 6. Statistics of the frequency and time-domain discrepancy of the final iteration compared with the desired values are shown in Table 3. Assessing Table 3 and Figs. 5 and 6, it is evident that the spectral error is very small (high $r^2_{S(f)}$ values), yet some minor discrepancy in the magnitude of crest and troughs is observed. In particular, there is notable error in the magnitude of the trough following the peak, $\epsilon_{\tau 2}$, yet errors in the preceding trough ($\epsilon_{\tau 1}$), crest amplitudes (ϵ_α), and asymmetry between troughs (Δ_τ) are below 10% in all cases. These discrepancies are discussed further in Section 4.1, whilst additionally assessing the influence of the turbine on the form of the NewWave groups.

The requirement for correction when generating NewWave groups in the presence of fast current is evidenced by the results of the first iteration (Figs. 5 and 6). Significant under-production of the energy content and large error in phase, highlighted by the mismatch in crest time, are observed. These effects are

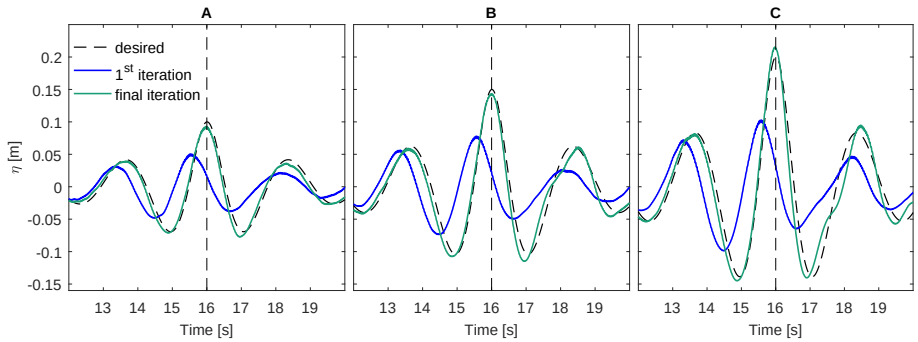

Figure 5: Time-series outputs of the iterative NewWave correction procedure

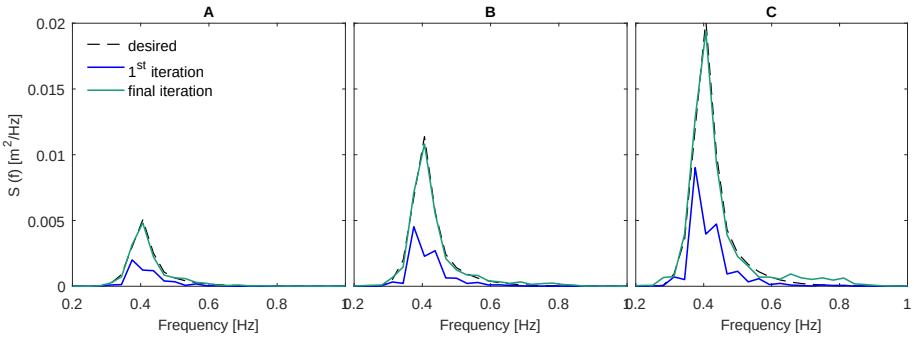

Figure 6: Spectral outputs of the iterative NewWave correction procedure

due to wave-current interaction and in following-current conditions, this causes reduced amplitude and increased wave group velocity across all frequencies. The initial focusing ability is hampered by the frequency-dependent modification of wave phase.

3.2. Time-Domain Turbine Response to NewWave Groups

The time-domain response of key turbine parameters to 5 repeats of the NewWave groups are shown in Fig. 7. To aid visualisation of the wave-induced effects a low pass filter, set at 4 Hz was applied. It is clear from this figure that the NewWave profile induces large variations in TST loads and power. Good agreement was found between the rotor thrust, shown in Fig. 7, and the foundation based measurements of F_X & M_Y. F_X & M_Y were consistently larger than the rotor measured thrust due to drag on the tower. Additionally, since the turbine nacelle is located at $z = 1$ m (see Fig. 4), M_Y and F_X were almost equivalent, with differences resulting from wave attenuation with depth. To aid visualisation, only the time-series of the rotor thrust is shown in the figure. However, comparisons are made between the three parameters in Section 3.4. The streamwise velocity, shown in Fig. 7, was measured 2D upstream of the

Table 3: Coefficient of determination, $r^2_{S(f)}$, between desired and generated NewWave spectrum and resulting time-domain discrepancies.

	Iteration process	**Time domain discrepancies**			
Reference	$r^2_{S(f)}$	$\epsilon_\alpha[\%]$	$\epsilon_{\tau 1}[\%]$	$\epsilon_{\tau 2}[\%]$	$\Delta_\tau[\%]$
A	0.986	5.8	3.4	12.3	8.7
B	0.994	3.3	3.7	10.9	7
C	0.993	8.6	4.9	1.99	2.7

turbine prior to wave group focusing. This results in wave-induced velocity components that are not in phase, resulting in peak velocities lower than those expected at the turbine location.

In Fig. 7 rotor averaged effects (power, thrust) are observed to be very repeatable. This highlights that, despite being a dynamic system, using NewWave to extract extreme wave-induced loads and moments is effective as their values are largely independent of system state. For individual blade loads this is not the case, as the measured RBM is a strong function of the blade angular position relative to the wave phase. Multiple repeats are therefore required to properly identify the expected wave-induced RBM variations. Further analysis is presented in Section 3.2.1 assessing the angular dependency of RBM.

3.2.1. Root bending moment

To enable effective understanding of the expected RBM as a function of angular position a number of repeats are required. The ability to generate multiple repeats of NewWave groups in short time frames enables this assessment to be carried out in a number of hours, rather than days. For these tests, logged encoder signals enable the absolute positions of the blades to be determined, which can be assessed in combination with the bending moments experienced by each blade. Fig. 8 shows the rotor position and corresponding root bending moments at the focus time for each of the 5 repeats of the largest NewWave: sea state C. It is evident in the majority of cases that, at the time of focus, the blade closest to top dead centre (TDC) experiences the largest bending moment, while the blade closest to the bottom dead centre (BDC) experiences the smallest. This is expected due to the decay of wave particle velocities with depth, providing larger wave-induced loads on the blades closer to the surface. It is shown that all blades, irrespective of angular position, experience a large increase in RBM at the focus point. Repeats 1 and 4 feature equivalent blade positions and show the most similarities in relative RBM values around the focus event.

The blade root bending moment as a function of angle for a specified wave phase (time) is shown in Fig. 9. This plot, in addition to the five tests discussed above, also includes the data from five further repeat tests (for each NewWave group) that lack torque and thrust measurements. Individual RBM – angle values are shown for times corresponding to wave crest and preceding trough. Ellipses have been fitted to the data to aid visibility. As expected, it is observed

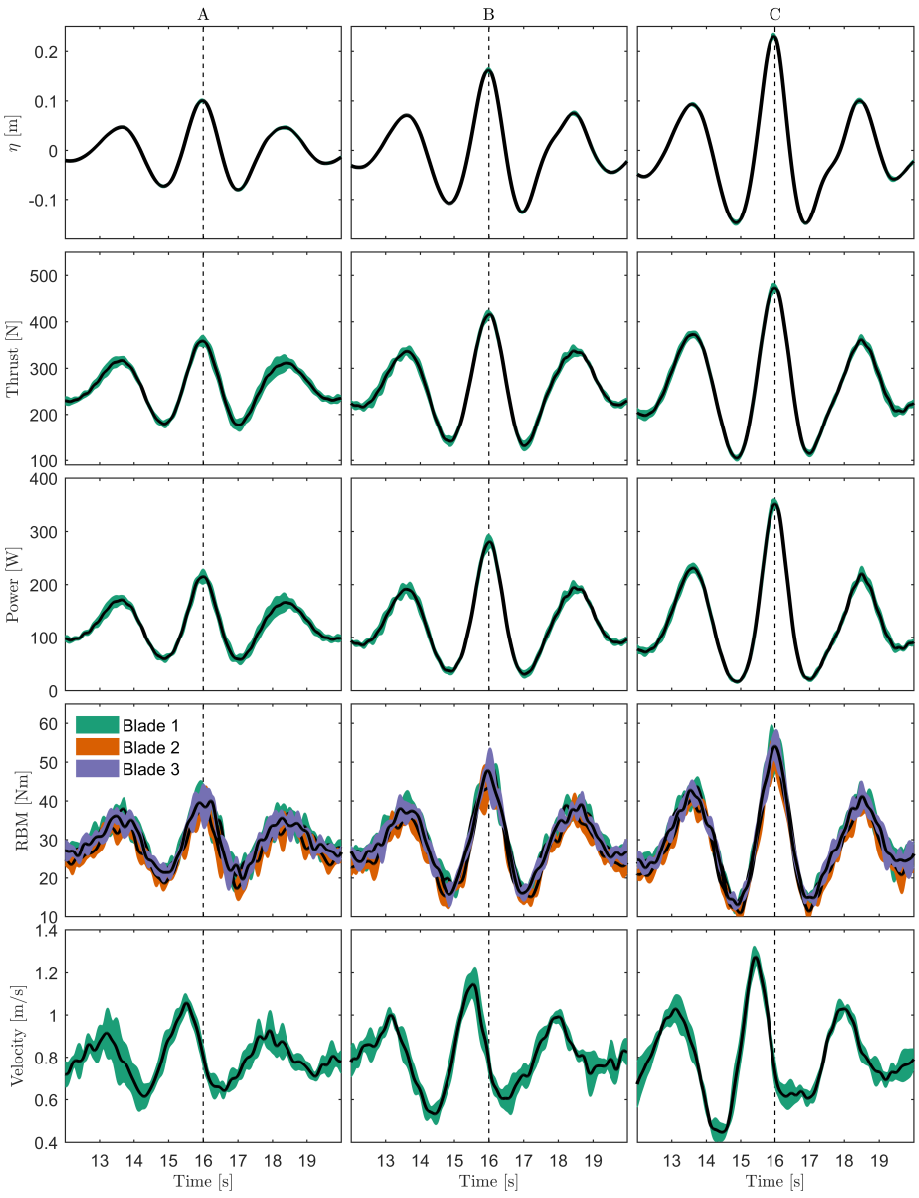

Figure 7: Time-series of turbine parameters resulting from NewWave focused wave groups. From top to bottom: surface elevation, thrust, power, RBM and streamwise velocity. Standard deviation of the 5 repeats is displayed using coloured filled-areas around the mean time-series (black)

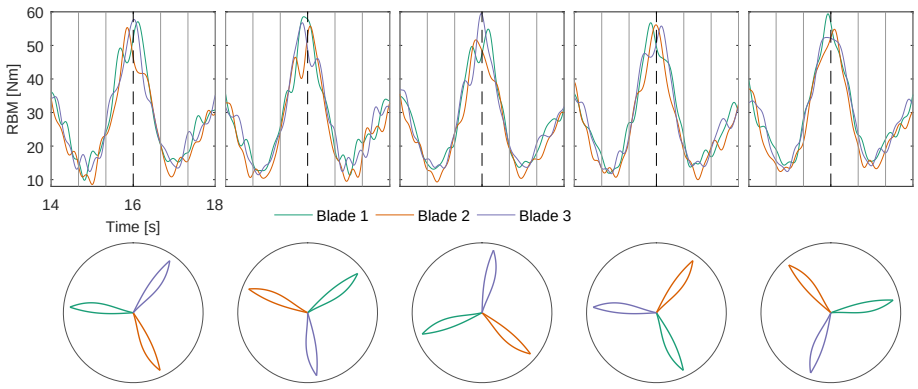

Figure 8: Bending moment shown for each blade over the 5 repeats for sea state C. The rotor position at the NewWave focus time is shown beneath each test. Grey vertical lines denote the instants at which the same rotor position applies i.e. once per turbine revolution.

that the larger NewWave groups cause increased variation in bending moment. At the trough, the wave-induced bending moment almost cancels out that produced from the current, and at the crest a large bending moment is observed regardless of angular position.

Larger moments are observed when blades are closer to TDC, with between 15-20% larger bending moment expected than at BDC for each of the NewWave groups presented. There will be a significant larger discrepancy for spectra with higher peak frequency as the wave-induced velocity attenuation with depth will be larger.

3.3. Frequency Domain Turbine Response to NewWave Spectra

Power spectral densities of key turbine and environmental parameters are shown in Fig. 10, and show the frequency domain equivalent of time domain extreme values of Fig. 7. A single Hanning window was applied to the time-series prior to evaluating power spectra. Together these plots indicate both extreme response to a short-duration extreme event as well as providing phase-averaged behaviour characteristic of input sea states. At frequencies where waves are present, the measured loads, power and streamwise velocity exhibit similar form to the surface elevation spectra. Outwith this range, turbine-based measurements also exhibit peaks at multiples of the rotational speed, $1p$ = 90 rpm = 1.5 Hz. Peaks at $1p$ and $2p$ are observed in the blade root bending moments as a result of both tower shadow and velocity shear, giving rise to $3p$ and $6p$ peaks in rotor averaged measurements: power and thrust. An additional peak at $12p$ is evident in the power, which is a result of motor cogging (12 poles) present in the measured torque. Although these rotation-driven-effects are important, from Fig. 10 it is evident that the wave induced fluctuations are extremely dominant, and in most cases are orders of magnitude larger.

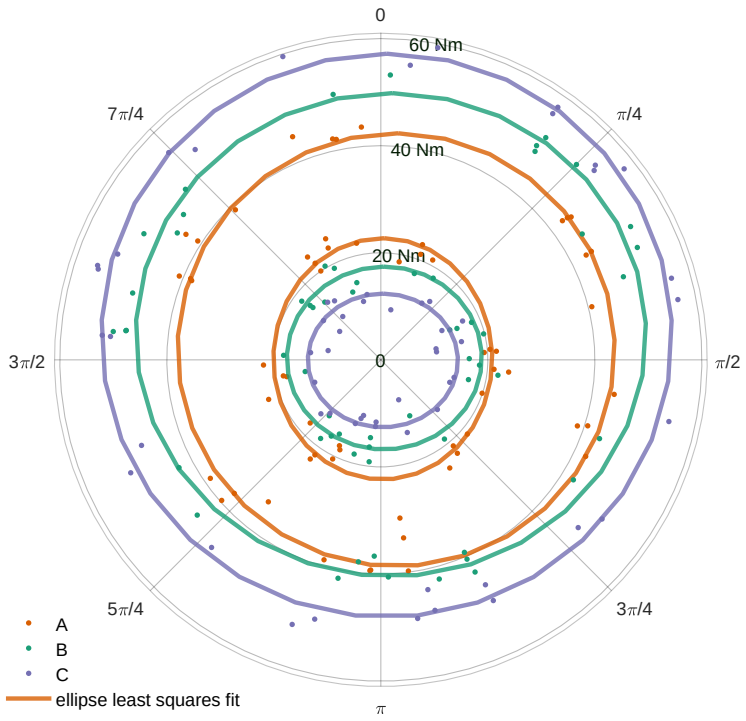

Figure 9: Instantaneous blade bending moment as NewWave crests (outer points) and troughs (inner points) pass over the turbine rotor. Shown as a function of angle, with fitted ellipses, for each of the three different amplitude NewWave groups.

3.4. Peak Loads and Power Fluctuations

As shown in Section 3.2, the NewWave groups introduce large fluctuations in the loads and power output of the speed controlled TST model. The magnitude of the peak loads and power fluctuations associated with expected extreme events have significant implications on the sizing and design of structural, electro-mechanical, and electrical components. The maximum wave induced loads and power fluctuations are shown in Fig. 11 as a function of measured NewWave crest amplitude. The presence of the turbine is observed to introduce a slight increase in the generated crest amplitude compared to empty-tank conditions (Fig. 5). This is discussed in Section 4.1.

It is evident from Fig. 11 that the NewWave conditions cause a large increase in loads and power output from the baseline current-only case. Full-scale equivalent values of these parameters, obtained using Froude scaling (see [29]), are given in Table 4, and put into perspective the peak values recorded during the test program. If the largest NewWave is deemed to be representative of a likely extreme condition, the foundation must be able to withstand a moment of 25.5 MNm, and the generator and power electronics must be able to deal with an instantaneous power surge of three times normal rated power.

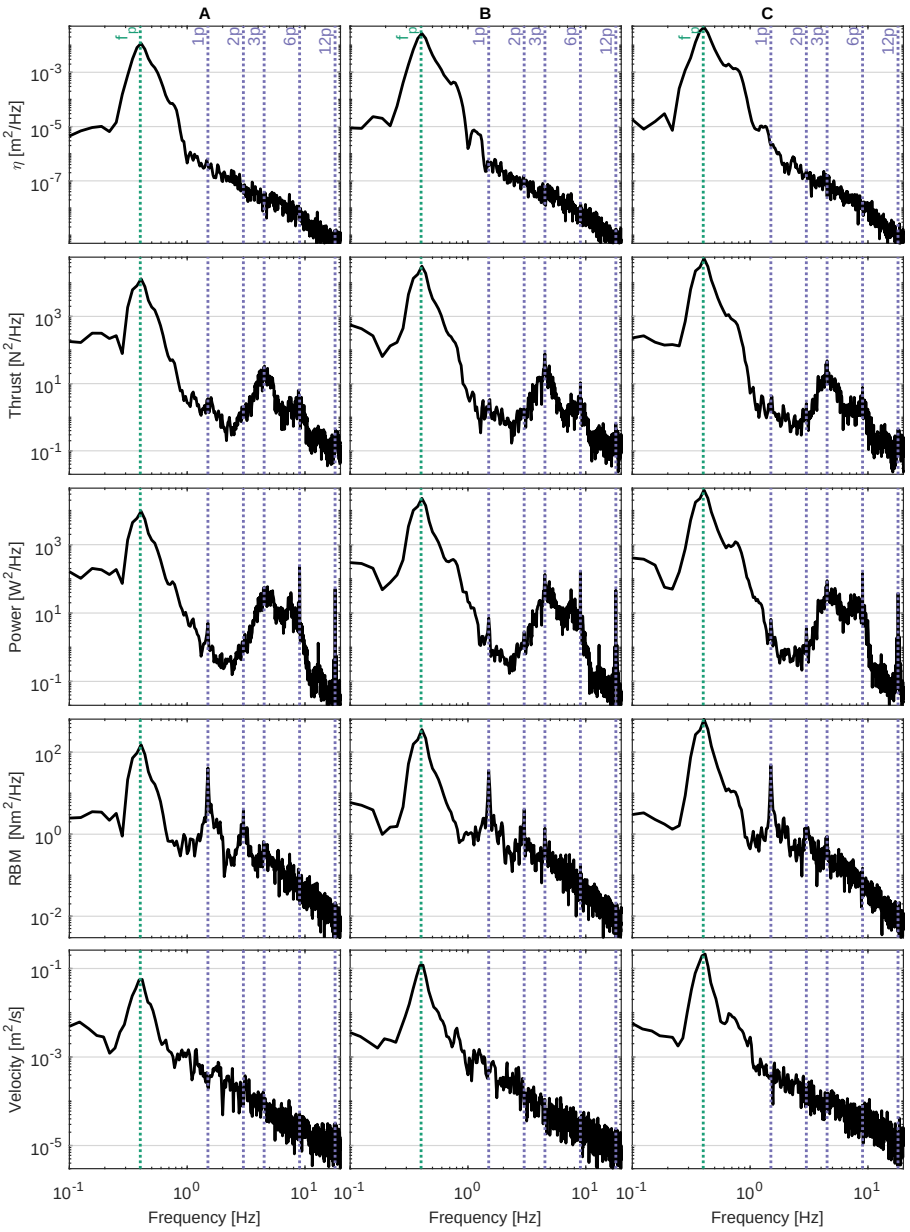

Figure 10: Power spectra of mean power, load, velocity and surface elevation resulting from NewWave focused wave groups. The peak wave frequency, and key multiples of the rotational speed are shown by dashed vertical lines.

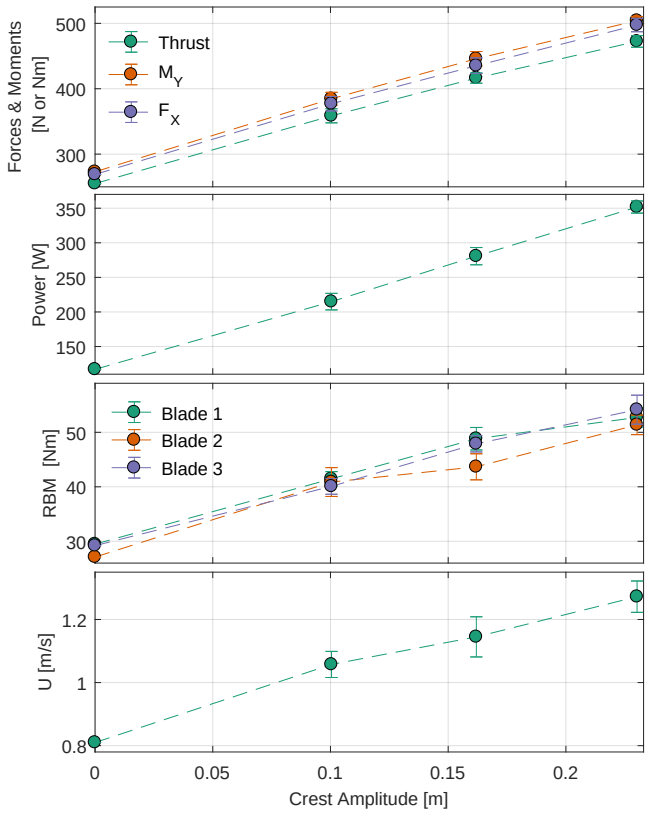

Figure 11: Peak values of turbine parameters from low-pass filtered time-series as a function of NewWave crest amplitude measured above the turbine. Mean value over the 5 repeats shown, with error bars representing the standard deviation between repeats. Equivalent full-scale values are presented in Table 4.

Table 4: Full-scale equivalent peak values of turbine parameters, from low-pass filtered time-series, as a function of NewWave crest amplitude measured above the turbine.

Reference	Crest [m]	Thrust [MN]	M_Y [MNm]	F_X [MN]	Power [MW]	RBM [MNm]	U [m/s]	W [m/s]
Current only	-	0.86	13.8	0.91	1.53	1.48	3.14	0.00
A	1.51	1.21	19.5	1.27	2.81	2.10	4.10	0.39
B	2.43	1.41	22.6	1.47	3.67	2.47	4.43	0.72
C	3.45	1.59	25.5	1.68	4.60	2.74	4.93	1.00

4. Discussion

The use of NewWave focused wave groups to assess extreme wave loadings on, and responses of, a horizontal axis tidal turbine was introduced in this paper. The response of the turbine model, in terms of loads and moments

experienced by the blades, rotor, and turbine structure, were found to be heavily influenced by the temporal and spectral form of the wave condition tested. By subjecting the turbine to focused NewWave wave groups, peak responses of the turbine are derived, which directly impact turbine design. Section 4.1 discusses the NewWave group design methodology presented with an emphasis on the correction procedure adopted. The impact of the turbine on the synthesis of NewWave groups and the generation of NewWave groups in opposing currents are examined. Section 4.2 discusses the application of NewWave groups as a design tool to develop turbine control strategies.

4.1. Generation of NewWave Groups in Energetic Currents

As detailed in Section 2.1.2, a correction procedure was implemented to create the defined NewWave conditions in the presence of a fast current, with corresponding outputs shown in Section 3.1. The characterised wave profiles exhibit minor variation from those targeted which is to be expected given the significant and frequency dependent modification to waves introduced by the presence of fast currents. Section 4.1.1 and Section 4.1.2 discuss, respectively, the increase in the measured crest amplitudes when the turbine is present (as observed in Section 3.2) and the issues encountered in the creation of NewWave in opposing currents.

4.1.1. Turbine Influence on NewWave Profile

The presence of the turbine model increased crest amplitudes, as shown in Fig. 12. Turbine-induced upstream flow retardation (compared to the empty-tank case) result in generated waves experiencing reduced modification by the current on approach to the turbine. It was anticipated that for the following wave conditions the upstream velocity change introduced by the turbine would be insignificant (unlike the opposing-current case where wave groups arrive at the turbine rotor plane having transited the length of the turbine wake). Whilst the under-estimation of this effect led to larger than specified crest amplitudes, the form of the focused groups remains representative of the intended NewWave profile. Updated frequency and time-domain discrepancies are presented in Table 5, and display the equivalent parameters to those detailed in Table 3. These wave statistics, incorporating the effect of the presence of the turbine model, have been used to contextualise the resulting turbine response (see Table 4 and Figs. 7 and 11).

Table 5: Coefficient of determination between desired and generated NewWave spectrum and resulting time-domain discrepancies with the turbine present.

	Spectral Error	**Time domain discrepancies**			
Reference	$r^2_{S(f)}$	$\epsilon_\alpha[\%]$	$\epsilon_{\tau 1}[\%]$	$\epsilon_{\tau 2}[\%]$	$\Delta_\tau[\%]$
A	0.942	0.44	5.3	16	9.9
B	0.927	8.0	3.5	21	17
C	0.941	15	6.4	7.1	0.68

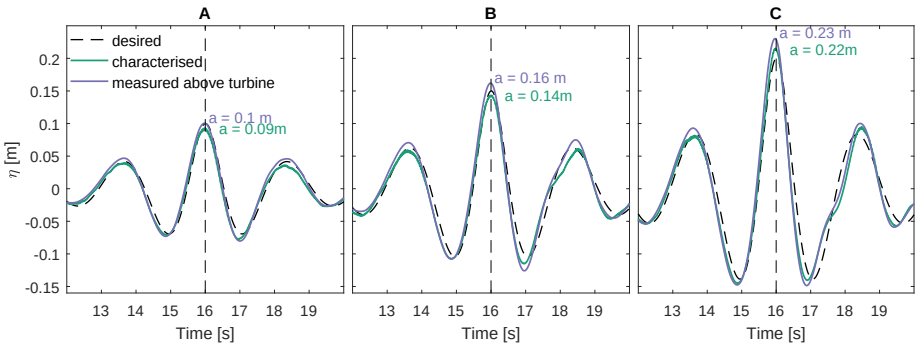

Figure 12: Effect of turbine on the synthesis of NewWave groups

With the turbine present, overall discrepancies in the NewWave profile from the target are larger. However, some improvements are seen, particularly to the crest amplitude of NewWave group A and trough symmetry of group C. NewWave B now exhibits significant trough asymmetry either side of the focused crest yet all measured troughs preceding the focal events remain close to desired values. There is also a large increase in crest amplitude noted for sea state C, yet this group now exhibits remarkable symmetry in trough amplitudes and can be effectively described by a larger NewWave spectrum. Surface elevations were found to be highly repeatable with the turbine present, suggesting sea state correction can, in future, be carried out with the model pre-installed. This approach will reduce trough asymmetries and amplitude error. Furthermore, this method will be of critical importance when generating opposing waves over the wake of a turbine.

4.1.2. Re-creating NewWave Groups in Fast Opposing Currents

A tidal turbine exposed to conditions where waves and currents have opposing directions represents an important extreme load case. The generation of opposing NewWave groups was therefore trialled. Their generation was found to be challenging and results show unacceptably large discrepancy from the target wave profile. Difficulties stem from the waves being heavily modified by the fast opposing current, creating waves with increased steepness and reduced velocity. This results in NewWave groups that deviate significantly from the desired wave heights and phases, and requires the implementation of a large number of iterations to approach the desired conditions. This is highlighted in Fig. 13, where 15 iterations were required to achieve a wave group similar to the target spectrum and time-series. This aspect, however, can be overcome by using previous empirical phase and wave height corrections as starting points to the iterative procedure.

Moreover, flow turbulence further hampers the generation of well-formed NewWave groups in fast opposing currents. Turbulent intensities (TI) are typically around 5-11% in the FloWave tank [30]. These stochastic velocity pertur-

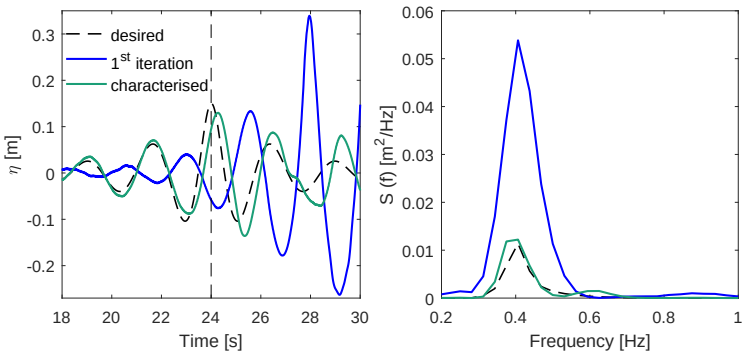

Figure 13: Time-series and frequency spectra of attempting to correct NewWave group in 0.8 m/s opposing current. Shown in the first and fifteenth iteration (characterised).

bations around the mean 0.8 m/s flow represent a significant proportion of the group velocity of the travelling wave components, which have been lowered by the opposing current, and thus introduce a large and unpredictable alteration to both the wave height and phase. This makes the correction process difficult and unstable, leading to low repeatability even with a well 'characterised' sea state. The form and repeatability of NewWave groups in opposing current will improve with reduced current velocity and reduced TI values. At a flow speed of 0.8 m/s and with the inherent TI values present in the absence of flow conditioning it was deemed not achievable at present.

4.2. Application of NewWave as a TST Design Tool

Using NewWave groups provides a fast, repeatable and effective method to study extreme wave loadings on tidal turbines, and is demonstrated in this paper in the presence of fast currents representative of tidal stream sites. This demonstrated ability enables NewWave groups to be used as a design tool for refining tidal turbine design and their corresponding control strategies. To further validate this approach, development work is being undertaken to enable comparison of extreme wave-induced loads obtained using focused wave groups to those measured in long-run irregular wave tests.

Tidal turbine control plays an important role in determining the performance of the turbine and the loading of the different parts of the turbine during extreme wave events. The power output of fixed-pitch turbines are often regulated in fast flow conditions [31, 32, 33, 34]. At extreme flow speeds the turbines are sometimes mechanically braked, producing no power. Under these operating conditions, and when a less stiff speed control or torque control are used, the loading on the different parts of the turbine will be markedly different compared to when the turbine is normally operating. The fluctuations in the power generation profile of the turbine under extreme wave events, which impact the electricity network into which this power is injected, are also heavily influenced by turbine control. Using NewWave groups permits efficient testing of different

turbine control strategies during extreme wave events and also facilitates fast optimisation of these control strategies to meet various structural or electricity network demands.

To demonstrate the presented methodology, three example NewWave groups in fast following current were created and used to impart combined wave-current loads on the TST model. The design procedure for creating these conditions can be used to synthesise NewWave groups with wave heights and periods associated with site-specific extreme wave conditions. This approach can also be extended to study extreme wave loadings on different turbine types, using alternative variants of turbine control algorithms and operating in different flow conditions. This will include applications with faster following current conditions and opposing currents if the velocity can be reduced or turbulence levels are reduced via flow conditioning. In early commercial tidal farms of bed mounted devices, structural and station keeping costs will contribute to more than 25% of the farm's indicative levelised cost of energy [35]. Any savings that can be made on the structure, obtained by a better understanding of turbine loads under various flow, wave, and turbine control regimes, will benefit the industry.

5. Conclusions

Extreme waves can induce catastrophic loads on offshore structures and energy devices, and as such they are an important environmental factor to de-risk maritime equipment, including tidal turbines. To this end, a variety of extreme wave conditions were re-created using NewWave focused wave groups, and used to test a fully instrumented 1:15 scale tidal turbine. The methodology used to create NewWave groups in current is shown to be effective, and three wave conditions were created in 0.8 m/s of following current. The creation of equivalent NewWave groups in opposing current were found not to be achievable as the phases of the slow travelling wave components were unpredictably altered by turbulent velocity fluctuations.

The response of the turbine model to the focused wave groups is shown to be very significant, and loads and power fluctuations are found to strongly mimic both the temporal and spectral form of the generated wave conditions. In a full-scale crest amplitude of 3.45 m, peak tower bending moments of 25.5 MNm (from 13.8 MNm in current alone) are identified, along with power fluctuations of three times nominal rated power. These results highlight the large influence extreme waves have on tidal turbine response, which has significant implications for the design and operation of both individual, and farms of, tidal turbines.

This work demonstrates an extension of the NewWave method for use in energetic currents, which subsequently enables focused wave groups to be used to assess tidal turbines in extreme wave-current conditions. The results presented demonstrate that both are achievable, and that this approach can be utilised as an effective tool for the de-risking and development of tidal turbines.

Acknowledgements

The authors are grateful for financial support from the U.K. Engineering and Physical Sciences Research Council through FloWTurb: Response of Tidal Energy Converters to Combined Tidal Flow, Waves and Turbulence (EP/N021487/1) and SuperGen UK Centre for Marine Energy Research (EP/M014738/1). The authors also acknowledge support from the EPSRC for funding the FloWave Ocean Energy Research facility (EP/I02932X/1). The authors are extremely grateful to the staff at the FloWave facility, in addition to the FloWTurb project team, for making this research possible.

Author Contributions

Sam Draycott designed and conducted the hydrodynamic aspects of testing and led the subsequent data analysis. Anup Nambiar assembled, commissioned and operated the model tidal stream turbine along with Brian Sellar who also co-developed the FloWTurb project. Tom Davey provided research software and contributed to the article review. Venugopal Vengatesan, the Principal Investigator of the FloWTurb project, was involved in the original test specification and supported this specific article by providing internal review.

References

[1] The Crown Estate, UK Wave and Tidal Key Resource Areas Project - Summary Report, Tech. rep. (2012).

[2] Atlantis, MeyGen — Tidal Projects — Atlantis Resources, https://www.atlantisresourcesltd.com/projects/meygen/ (2017). URL https://www.atlantisresourcesltd.com/projects/meygen/

[3] S. Draper, T. A. A. Adcock, A. G. L. Borthwick, G. T. Houlsby, Estimate of the tidal stream power resource of the Pentland Firth, Renewable Energy 63 (2014) 650–657. doi:10.1016/j.renene.2013.10.015.

[4] I. A. Milne, R. N. Sharma, R. G. J. Flay, S. Bickerton, The Role of Waves on Tidal Turbine Unsteady Blade Loading, in: Proceedings of the 3rd International Conference on Ocean Energy, 2010, pp. 1–6.

[5] J. MacEnri, M. Reed, T. Thiringer, Influence of tidal parameters on SeaGen flicker performance, Philosophical Transactions of the Royal Society of London A: Mathematical, Physical and Engineering Sciences 371 (1985). doi:10.1098/rsta.2012.0247.

[6] I. A. Milne, R. N. Sharma, R. G. J. Flay, The structure of turbulence in a rapid tidal flow, Proceedings of the Royal Society of London A: Mathematical, Physical and Engineering Sciences 473 (2017). doi:10.1098/rspa.2017.0295.

[7] Marine energy - Wave, tidal and other water current converters. Part 201: Tidal energy resource assessment and characterization, Standard, International Electrotechnical Commission, Geneva, Switzerland (2015).

[8] Marine energy - Wave, tidal and other water current converters. Part 200: Electricity producing tidal energy converters - Power performance assessment, Standard, International Electrotechnical Commission, Geneva, Switzerland (2013).

[9] Marine energy - Wave, tidal and other water current converters. Part 2: Design requirements for marine energy systems, Standard, International Electrotechnical Commission, Geneva, Switzerland (2016).

[10] P. S. Tromans, A. R. Anatruk, P. Hagemeijer, New Model for the Kinematics of Large Ocean Waves Application as a Design Wave, in: Proceedings of the First International Offshore and Polar Engineering Conference, Vol. 8, 1991, pp. 64–71.

[11] L. Xu, N. Barltrop, Health and Safety Executive of Great Britain, Wave Slap Loading on FPSO Bows, Research report (Great Britain. Health and Safety Executive), HSE Books, 2005.

[12] L. Xu, N. Barltrop, B. Okan, Bow impact loading on FPSOs 1-Experimental investigation, Ocean Engineering 35 (11-12) (2008) 1148–1157. doi:10.1016/j.oceaneng.2008.04.013.

[13] S. Draycott, D. Sutherland, J. Steynor, B. Sellar, Re-Creating Waves in Large Currents for Tidal Energy Applications, Energies 10 (2017) 1838. doi:10.3390/en10111838.

[14] S. Draycott, J. Steynor, T. Davey, D. M. Ingram, Isolating incident and reflected wave spectra in the presence of current, Coastal Engineering Journal (2018) 1–12.

[15] M. J. Cassidy, R. E. Taylor, G. T. Houlsby, Analysis of jack-up units using a Constrained New Wave methodology, Applied Ocean Research 23 (2001) pp. 221–234. doi:10.1016/S0141-1187(01)00005-0.

[16] J. R. Grice, P. H. Taylor, R. E. Taylor, Second-order statistics and designer waves for violent free-surface motion around multi-column structures, Philosophical Transactions of the Royal Society of London A: Mathematical, Physical and Engineering Sciences 373 (2033) (2015) 20140113. doi:10.1098/rsta.2014.0113.

[17] L. A. O. Neill, E. Fakas, M. Cassidy, A novel application of constrained NewWave theory for floatover deck installations, in: Proceedings of the 23rd International Conference on Offshore Mechanics and Arctic Engineering, 2004, pp. 1–10.

[18] M. Hann, D. Greaves, A. Raby, Snatch loading of a single taut moored floating wave energy converter due to focussed wave groups, Ocean Engineering 96 (2015) 258–271. doi:10.1016/j.oceaneng.2014.11.011.

[19] M. Hann, D. Greaves, A. Raby, B. Howey, Use of constrained focused waves to measure extreme loading of a taut moored floating wave energy converter, Ocean Engineering 148 (October 2017) (2018) 33–42. doi:10.1016/j.oceaneng.2017.10.024.

[20] D. Stagonas, E. Buldakov, R. Simons, Focusing unidirectional wave groups on finite water depth with and without currents, Coastal Engineering Proceedings 34 (2014) 3–8.

[21] I. G. Jonsson, C. Skougaard, J. D. Wang, Interaction between waves amd currents, Coastal Engineering Proceedings 1 (12).

[22] D. R. Noble, T. Davey, H. C. M. Smith, P. Kaklis, A. Robinson, T. Bruce, Characterisation of spatial variation in currents generated in the FloWave Ocean Energy Research Facility, in: Proceedings of the 11th European Wave and Tidal Energy Conference, Nantes, France, 2015, pp. 1–8.

[23] G. S. Payne, T. Stallard, R. Martinez, Design and manufacture of a bed supported tidal turbine model for blade and shaft load measurement in turbulent flow and waves, Renewable Energy 107 (2017) 312–326. doi:10.1016/j.renene.2017.01.068.

[24] S. Draycott, G. Payne, J. Steynor, A. Nambiar, B. Sellar, V. Venugopal, An experimental investigation into non-linear wave loading on horizontal axis tidal turbines, Journal of Fluids and Structures 84 (2019) 199–217. doi:10.1016/j.jfluidstructs.2018.11.004.

[25] T. Stallard, T. Feng, P. K. Stansby, Experimental study of the mean wake of a tidal stream rotor in a shallow turbulent flow, Journal of Fluids and Structures 54 (2015) 235–246. doi:10.1016/j.jfluidstructs.2014.10.017.

[26] D. Ingram, R. Wallace, A. Robinson, I. Bryden, The design and commissioning of the first, circular, combined current and wave test basin, in: Proceedigns of the OCEANS 2014, 2014, pp. 1–7. doi:10.1109/OCEANS-TAIPEI.2014.6964577.

[27] A. Robinson, D. Ingram, I. Bryden, T. Bruce, The generation of 3D flows in a combined current and wave tank, Ocean Engineering 93 (2015) 1–10. doi:10.1016/j.oceaneng.2014.10.008.

[28] K. Hasselmann, T. P. Barnett, E. Bouws, H. Carlson, D. E. Cartwright, K. Enke, J. A. Ewing, H. Gienapp, D. E. Hasselmann, P. Kruseman, A. Meerburg, P. Muller, D. J. Olbers, K. Richter, W. Sell, H. Walden, Measurements of Wind-Wave Growth and Swell Decay during the Joint

North Sea Wave Project (JONSWAP), Ergnzungsheft zur Deutschen Hydrographischen Zeitschrift Reihe A(8) (12) (1973) p.95.

[29] V. Heller, Scale effects in physical hydraulic engineering models, Journal of Hydraulic Research 49 (3) (2011) 293–306. doi:10.1080/00221686.2011.578914.

[30] D. R. J. Sutherland, D. R. Noble, J. Steynor, T. A. D. Davey, T. Bruce, Characterisation of Current and Turbulence in the FloWave Ocean Energy Research Facility, Ocean Engineering 139 (2017) 103–115. doi:10.1016/j.oceaneng.2017.02.028.

[31] K. Gracie-Orr, T. M. Nevalainen, C. M. Johnstone, R. E. Murray, D. A. Doman, M. J. Pegg, Development and initial application of a blade design methodology for overspeed power-regulated tidal turbines, International Journal of Marine Energy 15 (Supplement C) (2016) 140–155. doi:10.1016/j.ijome.2016.04.006.

[32] M. Harrold, P. Bromley, M. Broudic, D. Clelland, Demonstrating a tidal turbine control strategy at laboratory scale, in: Proceedings of the ASME 2016 35th International Conference on Ocean, Offshore and Arctic Engineering, 2016.

[33] M. Arnold, F. Biskup, P. W. Cheng, Load reduction potential of variable speed control approaches for fixed pitch tidal current turbines, International Journal of Marine Energy 15 (Supplement C) (2016) 175–190. doi:https://doi.org/10.1016/j.ijome.2016.04.012.

[34] B. Whitby, C. E. Ugalde-Loo, Performance of Pitch and Stall Regulated Tidal Stream Turbines, IEEE Transactions on Sustainable Energy 5 (1) (2014) 64–72. doi:10.1109/TSTE.2013.2272653.

[35] Carbon Trust, Accelerating marine energy - The potential for cost reduction - insights from the Carbon Trust Marine Energy Accelerator (2011) 1–51. URL https://www.carbontrust.com/media/5675/ctc797.pdf